Eur. Phys. J. B **58**, 411–421 (2007)
DOI: 10.1140/epjb/e2007-00250-0

THE EUROPEAN PHYSICAL JOURNAL B

High-order subharmonic parametric resonance of nonlinearly coupled micromechanical oscillators

J. Zhu, C.Q. Ru[a], and A. Mioduchowski

Department of Mechanical Engineering, University of Alberta, Edmonton T6G 2G8, Canada

Received 18 May 2007
Published online 22 September 2007 –

Abstract. This paper studies parametric resonance of coupled micromechanical oscillators under periodically varying nonlinear coupling forces. Different from most of previous related works in which the periodically varying coupling forces between adjacent oscillators are linearized, our work focuses on new physical phenomena caused by the periodically varying nonlinear coupling. Harmonic balance method (HBM) combined with Newton iteration method is employed to find steady-state periodic solutions. Similar to linearly coupled oscillators studied previously, the present model predicts superharmonic parametric resonance and the lower-order subharmonic parametric resonance. On the other hand, the present analysis shows that periodically varying nonlinear coupling considered in the present model does lead to the appearance of high-order subharmonic parametric resonance when the external excitation frequency is a multiple or nearly a multiple ($\geqslant$3) of one of the natural frequencies of the oscillator system. This remarkable new phenomenon does not appear in the linearly coupled micromechanical oscillators studied previously, and makes the range of exciting resonance frequencies expanded to infinity. In addition, the effect of a linear damping on parametric resonance is studied in detail, and the conditions for the occurrence of the high-order subharmonics with a linear damping are discussed.

PACS. 62.30.+d Mechanical and elastic waves; vibrations – 63.22.+m Phonons or vibrational states in low-dimensional structures and nanoscale materials

1 Introduction

Earlier researches on MEMS-related mechanics have mainly focused on mechanical behavior of individual components (such as a single microcantilever attracted by a rigid substrate) [1–4]. More recently, considerable attention has turned to collective mechanical behavior of coupled micromechanical systems. Especially, due to their relevance to MEMS/NMES [5–8], growing interest has been attracted to collective nonlinear dynamic behavior of large coupled micromechanical/nanomechanical systems, such as parametric resonance [9–12], and localized modes [13–16] of a coupled large array of interacting microbeams. In particular, Buks and Roukes [9,10] fabricated an array of 67 doubly clamped microbeams, in which all even-numbered beams are electrically connected to one electrode while all odd-numbered beams to another electrode. An electrical voltage applied between the two electrodes induces attracting electrostatic forces between side-faces of any two adjacent beams. This coupled microbeam system was driven parametrically by introducing a periodically varying ac component to the voltage applied between the two electrodes. The response of the microbeam array showed some interesting nonlinear phenomena. For example, as the exciting frequency of the periodically varying ac component was swept up, typical response consisted of a small number of wide peaks, instead of 67 resonance peaks predicted by the linear theory of parametric resonance. Using a perturbation theory, Lifshitz and Cross [11] studied and explained these nonlinear phenomena based on a model of linearly coupled array of nonlinear oscillators. More recently, Bromberg et al. [12] further studied parametric resonance of a large array of linearly coupled oscillators using a multiscale perturbation analysis.

Although time-independent nonlinear coupling forces between oscillators (characterized by nonlinear coupling terms of constant coefficients) has been studied extensively (see e.g. [16–18]), parametric resonance of coupled oscillators under periodically varying nonlinear coupling forces (characterized by nonlinear coupling terms of periodically-varying coefficients) has received much less attention [19,20]. For example, in the above-mentioned works on parametric resonance [9–12], the periodically varying coupling between any two adjacent microbeams is linearized and only elastic geometrical nonlinearity

[a] e-mail: c.ru@ualberta.ca

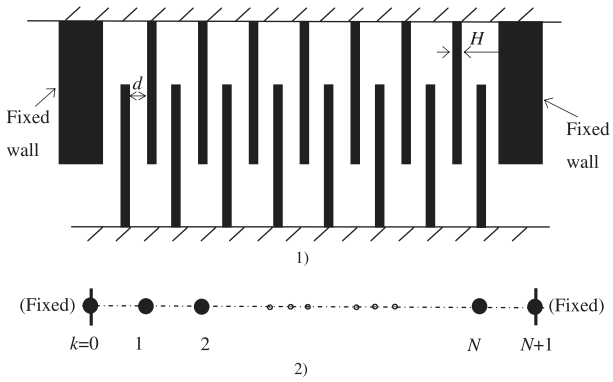

Fig. 1. Comb-drive microcantilever array and simplified spring model.

of the microbeams is taken into account. Also, most of previous works (except very few recent papers such as [19,20]) on parametric resonance of coupled oscillators, see e.g. [21–23], are limited to linearized coupling forces. No doubt, such a linearized coupling is reasonable for, say, the large array of doubly clamped microbeams studied in [8–11] where the thickness (0.25 μm) of beams is much smaller than the gap (4 μm) between adjacent beams and therefore the elastic nonlinearity of the doubly clamped microbeams is much more relevant than the nonlinear effect of coupling. However, in some other cases, such as comb-drive microcantilever array, shown in Figure 1-1), with a gap between adjacent beams comparable to or even smaller than the thickness of microcantilevers [24–30], elastic nonlinearity of microcantilevers is obviously much less relevant than the nonlinear dependency of the periodically varying coupling forces on the change in the gap between adjacent beams. In particular, in contrast to the elastic nonlinearity considered in [9–12] which leads to nonlinear terms of constant coefficients and has a stabilizing effect, the periodically varying coupling nonlinearity leads to nonlinear coupling terms of periodically-varying coefficients and has a destabilizing effect. This suggests that an oscillator system with periodically varying nonlinear coupling would more likely be parametrically excited than an oscillator system with elastic nonlinearity. Therefore, it is of great interest to study the effects of periodically varying nonlinear coupling on parametric resonance of coupled micromechanical oscillators.

The present work studies parametric resonance of nonlinearly coupled micromechanical oscillators under periodically varying coupling forces. Here, motivated by comb-drive microcantilevers mentioned above and the fact that elastic geometrical nonlinearity is much relevant for doubly clamped beams than cantilevers, we neglect the elastic nonlinearity of oscillators and focus on the role of periodically varying nonlinear coupling between adjacent oscillators. As will be shown in the present work, the periodically varying nonlinear coupling leads to some new physical phenomena which have not appeared in linearly coupled oscillators studied previously [9–12] and also have not been studied in previous related works [19,20]. Actually, the periodically varying nonlinear coupling studied in the present paper allows the appearance of high-order subharmonic parametric resonance when the excitation frequency is a multiple or nearly a multiple ($\geqslant$3) of one of the natural frequencies of the coupled oscillator system, although the conditions for the appearance of high-order subharmonic parametric resonance depend on the magnitude of linear damping.

2 Micromechanical oscillators with periodically varying nonlinear coupling

Let us consider a comb-drive microcantilever array, with the gap d between two side-faces of adjacent beams which is comparable to the thickness of beams H, as shown in Figure 1-1). For simplicity, just like [9–12], we shall assume that the first and the last beams are fixed and stationary. As a result, the complex end-effects, such as those studied in [29,30] for static pull-in instability of a parallel array of mutually attracting microbeams, will not appear in the present analysis. Furthermore, also like [9–12], it is assumed that each individual beam oscillates in its fundamental mode, and the simple spring (oscillator) model shown in Figure 1-2) will capture essential characteristics of the comb-drive microcantilever array.

Therefore, let us consider $(N+2)$ equally spaced oscillators of identical mass m and spring constant q, arranged along a straight line from $k=0$ (fixed left end) to $k=N+1$ (fixed right end), as shown in Figure 1-2). Let the displacement of the kth oscillator be X_k (because the left and right end oscillators are fixed, $X_0 = X_{N+1} = 0$). Assume that any two adjacent oscillators are attracted to each other through microscale surface forces, such as electrostatic, van der Waals or Casimir forces, given by $f = M/d^n$, where M represents the amplitude of the attractive forces which can be periodically varying, d is the distance between the two adjacent oscillators, and the index $n = 2$ (electrostatic force), =3 (van der Waals force), or =4 (Casimir force) [1–4]. Here, it should be stated that both van der Waals force and Casimir force share the same underlying physics, and thus the former is actually the short distance limit whereas the latter is the long distance limit of the same physical phenomenon. Thus, in the presence of a linear damping characterized by a constant viscous coefficient c, dynamics of the N mutually attracting oscillators is governed by

$$\frac{d^2x_k}{dt^2} + \frac{c}{m}\frac{dx_k}{dt} + \omega_0^2 x_k - \frac{M}{md_0^{n+1}}\left[\frac{1}{(1+x_{k+1}-x_k)^n} - \frac{1}{(1+x_k-x_{k-1})^n}\right] = 0,\ (k=1,2,\ldots,N) \quad (1)$$

where $x_k = X_k/d_0$ is dimensionless displacement of the kth spring, d_0 is the initial distance between adjacent springs,t is the time, and $\omega_0 = \sqrt{q/m}$ is the frequency of a single isolated spring in the absence of the spring-spring coupling with any other springs. Apparently, the equilibrium position defined by zero displacements x_k (or X_k) $= 0$ ($k = 1, 2, \ldots, N$) is a solution of (1), because

two attraction forces from two opposite sides are always equal and opposite for each of all intermediate oscillators ($k = 1, 2, \ldots, N$). However, non-zero solutions of (1) become possible when the coupling attractive forces characterized by $M(t)$ meet some conditions. In particular, appearance of any stable steady-state non-zero periodic solution in the neighborhood of the equilibrium position (of zero-displacements), under periodically varying $M(t)$ of a certain frequency, defines parametric resonance of the coupled oscillator system.

Natural frequencies of the coupled array of oscillators are determined by infinitesimal linear vibration of the coupled oscillators in the neighborhood of their equilibrium position x_k (or X_k) $= 0$ ($k = 1, 2, \ldots, N$). For infinitesimal displacements around the equilibrium position, linearized equation of (1) gives

$$\frac{d^2x_k}{dt^2} + \frac{c}{m}\frac{dx_k}{dt} + \omega_0^2 x_k - nQ\omega_0^2(2x_k - x_{k-1} - x_{k+1}) = 0, (k = 1, 2, \ldots, N) \quad (2)$$

where $Q = \frac{M}{qd_0^{n+1}}$ is the periodically varying loading parameter, defined based on the initial distance d_0. Thus, when M is a reasonably small positive constant, there exist N distinct natural frequencies of the linearized system (2) in the absence of the damping ($c = 0$), given by $\omega_i = \sqrt{1 - 4nQ\sin^2\frac{i\pi}{2(N+1)}}\omega_0$ ($i = 1, 2, \ldots, N$) [10]. For sufficiently large N, the highest natural frequency, ω_N, approaches ω_0. On the other hand, the lowest natural frequency, ω_1, reduces to zero when M increases gradually so that (nQ) reaches $1/4$, which indicates the existence of stationary non-zero solution and static instability of the coupled oscillator array, as studied in [29,30]. For example, for a large coupled oscillator array with two end oscillators fixed, such a static instability occurs when $Q = 1/8$ for $n = 2$, or $Q = 1/12$ for $n = 3$, or $Q = 1/16$ for $n = 4$.

Since comb-drive microcantilever arrays are usually electrostatically controlled [6–30], in what follows, we shall focus on the behavior of the coupled oscillators controlled by electrostatic forces ($n = 2$). Thus, when only a constant dc voltage V_{dc} is applied on the coupled oscillators, the N distinct natural frequencies of the linearized system are given by

$$\omega_i = \sqrt{1 - 8Q\sin^2\frac{i\pi}{2(N+1)}}\omega_0, \ (i = 1, 2, \ldots, N) \quad (3)$$

where $Q = \frac{\varepsilon_0 S V_{dc}^2}{2d_0^3 q}$, ε_0 is the permittivity of the medium between the beams, and S is the side-face area of adjacent beams exposed to the electrostatic filed. On the other hand, when a periodically varying ac voltage is added to the dc voltage, $V = V_{dc} + V_{ac}\cos(\Omega t)$, where V_{ac} and Ω are the amplitude and exciting frequency of the ac voltage, the amplitude of the nonlinear electrostatic force M will be periodically varying and given by

$$M = \frac{\varepsilon_0 S V^2}{2} = \frac{\varepsilon_0 S V_{dc}^2}{2}\left(1 + 2\frac{V_{ac}}{V_{dc}}\cos(\Omega t) + \left(\frac{V_{ac}}{V_{dc}}\right)^2\cos^2(\Omega t)\right). \quad (4)$$

Substituting (4) into (1), we obtain a dimensionless equation

$$\frac{d^2x_k}{d\tau^2} + \frac{c}{m\omega_0}\frac{dx_k}{d\tau} + x_k - Q\left[\frac{1}{(1 + x_{k+1} - x_k)^2} - \frac{1}{(1 + x_k - x_{k-1})^2}\right] \times \left[1 + 2\frac{V_{ac}}{V_{dc}}\cos\left(\frac{\Omega}{\omega_0}\tau\right) + \left(\frac{V_{ac}}{V_{dc}}\right)^2\cos^2\left(\frac{\Omega}{\omega_0}\tau\right)\right] = 0 \quad (5)$$

where $\tau = \omega_0 t$.

When the periodically varying coupling terms in (5) are linearized, the theory of classic Mathieu equation predicts that parametric resonance occurs when the frequency of the parametric excitation Ω is close to $2\omega_i/j$, where ω_i is any one of the N distinct natural frequencies defined in (3), and j is a positive integer [31,32]. In this case, because $\omega_i < \omega_0$ ($i = 1, 2, \ldots, N$), all resonance frequencies for parametric excitation will be bounded from above by $2\omega_0$, and then there will be no parametric resonance when the excitation frequency Ω is much higher than $2\omega_0$ when the coupling between adjacent oscillators is linearized [9–12].

In the present paper, we study the effect of periodically varying nonlinear coupling on parametric resonance, with particular interest in whether high-order subharmonic parametric resonance exists when the excitation frequency is close to a multiple ($\geqslant 3$) of one of the natural frequencies ω_i ($i = 1, 2, \ldots, N$). To this end, we shall seek, in the neighborhood of the equilibrium position, the lowest-order non-zero periodic solution of (5) with Ω/λ as the excited frequency, given by

$$x_k = a_k\cos\left(\frac{\Omega}{\lambda\omega_0}\tau\right) + b_k\sin\left(\frac{\Omega}{\lambda\omega_0}\tau\right) \quad (6)$$

where λ is an integer or the inverse of an integer, and a_k and b_k are some undetermined constants ($k = 1, 2, \ldots, N$). Using the harmonic balance method [32,33], we substitute (6) into (5), and then multiplying equation (5) by the functions $\cos(\frac{\Omega}{\lambda\omega_0}\tau)$ and $\sin(\frac{\Omega}{\lambda\omega_0}\tau)$ ($k = 1, 2, \ldots, N$), respectively, and integrating the resulting equation over $[0, 2\pi]$ lead to $2N$ nonlinear equations. The Newton iteration method is then employed to solve these equations for $2N$ unknown coefficients a_k and b_k ($k = 1, 2, \ldots, N$). In particular, the Newton iteration method with various initial values allows finding all possible solutions, and stability analysis of steady-state solutions (see Appendix) makes it possible to distinguish stable solutions from unstable ones. A non-zero stable solution of these nonlinear equations defines a parametric resonance characterized by a stable steady-state periodic solution of the form (6).

3 Parametric resonance without damping

In order to clearly demonstrate essential features of parametric resonance of nonlinearly coupled oscillators, let us

consider only three oscillators in which the middle one is nonlinearly coupled with two fixed end oscillators (thus $N = 1$ and $X_0 = X_2 = 0$, see Figure 1-2)). Actually, our results showed that a coupled system of more than three oscillators (with $N > 1$) exhibits essentially similar phenomena as the present simple system with $N = 1$ (the details will be reported elsewhere later). In this section, we first neglect the damping effect and consider $c = 0$. The effect of a linear damping will be studied in next section. In both sections, we take $Q = 1/20$ and $\frac{V_{ac}}{V_{dc}} = 0.1$ in equation (5). It then follows from (3) that $\omega_1 = 0.8944\omega_0$.

3.1 Parametric resonance with $\lambda \leqslant 2$

For the sake of comparison to previous related works with $\lambda \leqslant 2$ for linearly coupled oscillators [9–12], we first study the parametric resonance with $\lambda \leqslant 2$. Based on the harmonic balance method, as described above, we shall seek a periodic solution of the form (6) by solving 2 nonlinear equations for the two unknowns a_1 and b_1. The existence of a non-zero solution a_1 and b_1 defines a periodic solution of the intermediate oscillator nonlinearly coupled with two fixed end oscillators, and the periodic solution can be expressed as $x_1 = A_m \cos(\frac{\Omega}{\lambda\omega_0\tau} - \psi)$ (see Eq. (6)), where the amplitude $A_m = \sqrt{a_1^2 + b_1^2}$, and the phase $\psi = arctg(b_1/a_1)$.

Figure 2 shows the relationship between the amplitude of the excited resonance and the ac frequency Ω/ω_0 for parametric resonance defined by $\lambda = 0.5$, 1 or 2. In this figure and Figures 3–6, the dash lines represent unstable steady-state solutions, while the solid lines represent stable steady-state solutions. Detailed stability analysis of steady-state solutions is explained in Appendix. For example, steady-state solutions with $g(A_m^0, \psi^0) > 0$ are stable, while those with $g(A_m^0, \psi^0) < 0$ are unstable (see Eq. (A-15)). In particular, our results show that for $\lambda = 8$ and $c = 0$, the solutions with $\cos(8\psi^0) = -1$ are stable, while the solutions with $\cos(8\psi^0) = 1$ are unstable. Stability of the steady-state solutions with $\lambda = 0.5$, 1, 2, 3, 4 can be analyzed in a similar way (see Appendix).

Here, it should be stated that any point on the solid or dashed line would represent more than one solution which have the same amplitude but with different phases. In Figure 2-1), curves *a*) and *b*) intersect with the x-coordinate axis at point A ($\Omega/\omega_0 = 0.4451$) and B ($\Omega/\omega_0 = 0.4489$), respectively, and point C is the linear resonance frequency of $2\omega_1/j$ with $j = 4$, where $\omega_1 = 0.8944\omega_0$. In Figure 2-2), the coordinate of point A or B is $\Omega/\omega_0 = 0.8936$ or 0.8942, respectively, and point C is the linear resonance frequency of $2\omega_1/j$ ($=0.8944\omega_0$ with $j = 2$). In Figure 2-3), the coordinate of point A or B is $\Omega/\omega_0 = 1.7654$ or 1.81, and point C is the linear resonance frequency of $2\omega_1/j$ ($=1.7888\omega_0$ with $j = 1$). In particular, our results show that points A and B will approach point C when V_{ac}/V_{dc} approaches zero.

Similar to the responses of a parametrically excited Duffing oscillator [32] and electrostatical microelectromechanical oscillators with cubic nonlinear coupling [19,20], the response of the present system (5) also exhibits hysteresis phenomenon. For example, it is seen from Figure 2 that when the ac frequency Ω/ω_0 is higher than the coordinate of point B (say, 1.81 for $\lambda = 2$), only the (stable) trivial solution exists. When the ac frequency is between the coordinates of points A and B (say, $1.7654 \leqslant \Omega/\omega_0 \leqslant 1.81$ for $\lambda = 2$), the trivial solution is unstable, and the only stable solution is the periodic solution shown by the solid line in Figure 2. When the ac frequency Ω/ω_0 is less than the coordinate of point A (say, 1.7654 for $\lambda = 2$), two stable solutions exist, including the trivial solution and a stable steady-state solution shown by the solid line in Figure 2. Thus, when the ac frequency Ω/ω_0 decreased gradually from a bigger value (for example, more than 1.81), the amplitude of parametric resonance will increase along the solid line in Fig. 2-3). On the other hand, when the ac frequency increased gradually from a smaller value (for example, less than 1.7654), there will be no parametric resonance until Ω/ω_0 reaches point A (=1.7654) at which the response will jump abruptly to the solid line in Fig. 2-3) and gradually decrease to zero along this solid line.

All of these results on the stable and unstable steady-state solutions shown in Figure 2 for parametric resonance with $\lambda \leqslant 2$ are qualitatively similar to those obtained in [9–12] based on linearly coupled oscillators and those obtained in [19,20] based on oscillators with a cubic nonlinear coupling, around the linear resonance frequencies $\Omega = 2\omega_1/j$ ($j = 1$, 2 or 4).

3.2 Parametric resonance with $\lambda \geqslant 3$

Different from the previous works [9–12] and [19,20] which only focused on parametric resonance with $\lambda \leqslant 2$, the present work is particularly interested in existence of high-order subharmonic parametric resonance with $\lambda \geqslant 3$, which is equivalent to a resonance frequency around $\Omega = 2\omega_1/j$ with $0 < j < 1$.

Figure 3 shows the relationships between the amplitude of the excited resonance and the ac frequency for $\lambda = 3$, 4 or 8. In Figure 3-1), the solid line represents a stable steady-state solution, while an unstable steady-state solution also exists and is showed in Figure 3-1) by a dashed line which is almost coincident with the solid line and thus is covered by the solid line. Here, it should be stated that any point on the solid or dashed line would represent more than one solution which have the same amplitude but with different phases. The solution curves intersect with the x-coordinate axis at point $A(\Omega/\omega_0 = 2.6816)$ which approaches point C when V_{ac}/V_{dc} approaches zero, where the coordinate of point C is $\lambda\omega_1/\omega_0 = 2.6832$ with $\lambda = 3$ (equivalent to $\Omega = 2\omega_1/j$ with $j = 2/3$). In Figure 3-2), the two solution curves intersect with the x-coordinate axis at point A ($\Omega/\omega_0 = 3.5756$) which approaches point C when V_{ac}/V_{dc} approaches zero, where the coordinate of point C is $\lambda\omega_1/\omega_0 = 3.5776$ with $\lambda = 4$ (equivalent to $\Omega = 2\omega_1/j$ with $j = 1/2$). Similar to Figure 3-1) for $\lambda = 3$, the dashed line in Figure 3-3) for the unstable solution with $\lambda = 8$ is almost coincident with the solid line and thus is covered by the solid one. The solution

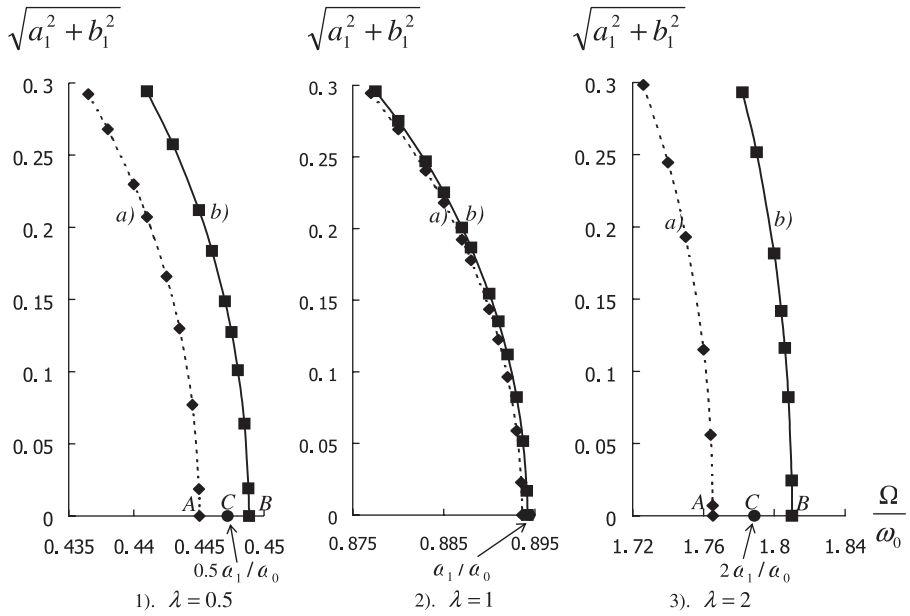

Fig. 2. Parametric resonance for $\lambda \leqslant 2$ without the viscous effect when $Q = \frac{\varepsilon_0 S V_{dc}^2}{2 d_0^3 q} = 1/20$ and $\frac{V_{ac}}{V_{dc}} = 0.1$ (solid line: stable steady-state solutions; dashed line: unstable steady-state solutions).

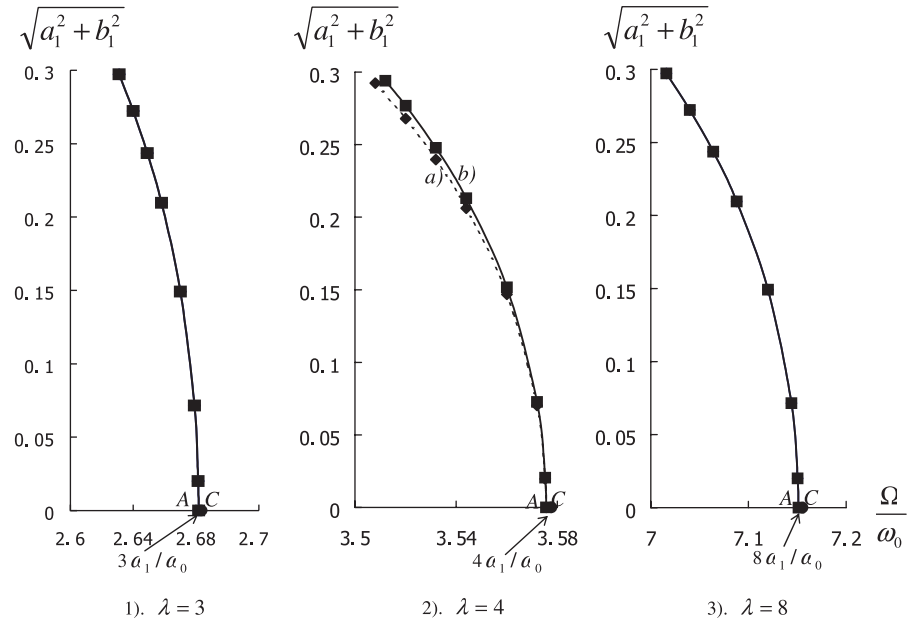

Fig. 3. Parametric resonance for $\lambda \geqslant 3$ without the viscous effect when $Q = \frac{\varepsilon_0 S V_{dc}^2}{2 d_0^3 q} = 1/20$ and $\frac{V_{ac}}{V_{dc}} = 0.1$ (solid line: stable steady-state solutions; dashed line: unstable steady-state solutions).

curves intersect the x-axis at point A ($\Omega/\omega_0 = 7.1512$) which approaches point C when V_{ac}/V_{dc} approaches zero, where the coordinate of $C = \lambda\omega_1/\omega_0 = 7.1552$ with $\lambda = 8$ (equivalent to $\Omega = 2\omega_1/j$ with $j = 1/4$).

It is seen from Figure 3 that near point A, small-amplitude stable steady-state periodic solutions exist for $\lambda = 3$, 4 or 8, in the neighborhood of the equilibrium position of the oscillators. Therefore, infinitesimal disturbances could lead to dynamic instability of the equilibrium position and the appearance of high-order subharmonic parametric resonance when the ac frequency is close to point A at which $\Omega = 2.6816\,\omega_0$ for $\lambda = 3$, or $\Omega = 3.5756\,\omega_0$ for $\lambda = 4$, or $\Omega = 7.1512\,\omega_0$ for $\lambda = 8$. These values of the resonance frequency Ω are very close to $\lambda\omega_1$, with a very small gap less than 0.1% for $\lambda = 3$, 4 or 8. Furthermore, our results (the details are omitted here) showed that similar high-order subharmonic parametric resonance also occurs for λ larger than 8. Therefore, in contrast to previous related works [9–12, 19,20] which showed the existence of lower-order subharmonic parametric resonance ($\lambda \leqslant 2$), the present work shows that periodically varying nonlinear coupling in

the nonlinearly coupled micromechanical oscillators does cause high-order subharmonic parametric resonance when the ac frequency is close to a multiple (say, 3, 4, 8 or more) of one of its natural frequencies.

In connection with this, we noticed that similar high-order subharmonic parametric resonance of specific order has been reported previously for a few damping-free nonlinear oscillators with periodically varying nonlinear powers of specific order [34,35]. These previous works (such as [34,35]) indicated that if the periodically varying nonlinear term of the governing equation is a power of order (λ–1), then subharmonic parametric resonance of order λ will exist while subharmonic parametric resonance of order higher than λ will not exist. Since the present model includes a general periodically varying nonlinear term (see the fourth term on LHS of (5)) whose Taylor series contains all orders of powers, the system studied in the present paper is expected to exhibit subharmonic resonances of all orders (such as λ = 3, 4, 8, or more), as shown by the above numerical results. In fact, our numerical results have confirmed that if the fourth term on LHS of (5) is expanded only up to the 7th power, subharmonic parametric resonance of order 8 will exist while subharmonic parametric resonance of order 9 will not exist. On the other hand, if the fourth term on LHS of (5) is expanded up to the 9th power, subharmonic parametric resonance of order 9 will exist. Therefore, our results are well consistent with the earlier works [34,35]. In particular, as stated in [34], theoretical results of [34] have been well confirmed experimentally.

4 Effects of the damping on parametric resonance

Next, let us study the effect of a linear damping on parametric resonance of the coupled micromechanical oscillators under periodically varying coupling forces. The parameters used in this section are $Q = 1/20$ and $V_{ac}/V_{dc} = 0.1$ (same as those in Sect. 3), but with a non-zero viscous coefficient $c > 0$.

4.1 Parametric resonance with $\lambda \leqslant 2$

Firstly, let us consider the parametric resonance with $\lambda \leqslant 2$, with increasing viscous coefficient c. It is found that for $\lambda \leqslant 2$, when the viscous coefficient is sufficiently small, there are still two different solution curves (one represents the stable steady-state solution, and the other represents the unstable one) which meet the x-coordinate axis at two distinct points, and these two solution curves change smoothly with increasing viscous coefficient. However, after the viscous coefficient reaches a certain critical value, the two solution curves will originate from some points above the x-axis and no longer meet the x-axis. Hence, the critical viscous coefficient can be defined as the smallest viscous coefficient beyond which no more periodic solution with vanishingly small amplitude exists. The critical viscous coefficient defined in this way for $\lambda = 0.5$, 1, 2, 3, 4, or 8 is shown in Table 1. In particular, the critical viscous coefficient for $\lambda \geqslant 3$ is always zero, which could mean that high-order subharmonic parametric resonance with vanishing small amplitude will not exist in the presence of an even small linear damping.

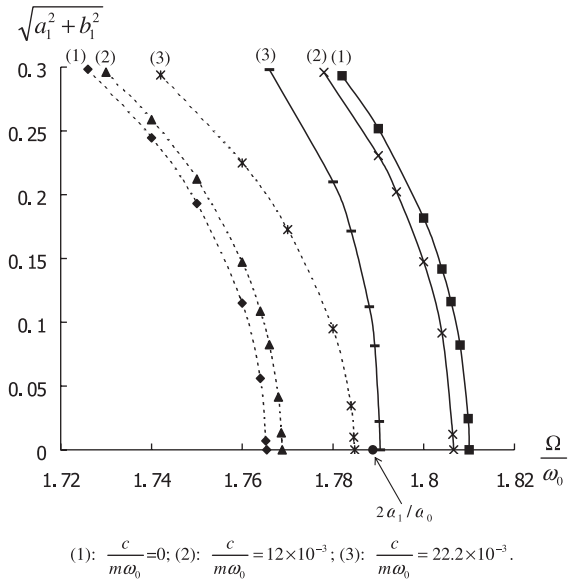

Fig. 4. Parametric resonance for $\lambda = 2$ with the viscous coefficient less than (or equal to) the critical value when $Q = \frac{\varepsilon_0 S V_{dc}^2}{2d_0^3 q} = 1/20$ and $\frac{V_{ac}}{V_{dc}} = 0.1$, where the critical value is $\frac{c}{m\omega_0} = 22.2 \times 10^{-3}$ for $\lambda = 2$ (solid line: stable steady-state solutions; dashed line: unstable steady-state solutions).

For $\lambda = 2$, the relationship between the amplitude of the excited periodic solution and the ac frequency is shown in Figure 4 when the viscous coefficient is less than (or equal to) the critical value (22.2×10^{-3}). In Figure 4, curve (1) represents the steady-state solutions without the damping effect (shown in Fig. 2-3)), and curve (2) or (3) represents the solutions with the viscous coefficient $\frac{c}{m\omega_0} = 12\times10^{-3}$, or 22.2×10^{-3} (the critical value). It is seen from Figure 4 that all stable solution curves originate from some points on the x-axis with zero-amplitude. Thus, when the viscous coefficient is less than (or equal to) the critical value, small-amplitude non-zero stable periodic solutions exist in the neighborhood of the equilibrium position, and infinitesimal disturbances can cause dynamic instability of the equilibrium position and parametric resonance of the coupled oscillators.

When the viscous coefficient is bigger than the critical value, the relationship between the amplitude of the excited periodic solution and the ac frequency for $\lambda = 2$ is shown in Figure 5. Different than Figure 4, the two solution curves shown in Figure 5 originate from a point A which is above the x-axis and associated with non-zero amplitude. Since the stable solution curves do not intersect with the x-coordinate axis, instability of the equilibrium position will lead to a periodic oscillation of the oscillators with small but finite amplitude. If the smallest amplitude, which is determined by point A in Figure 5,

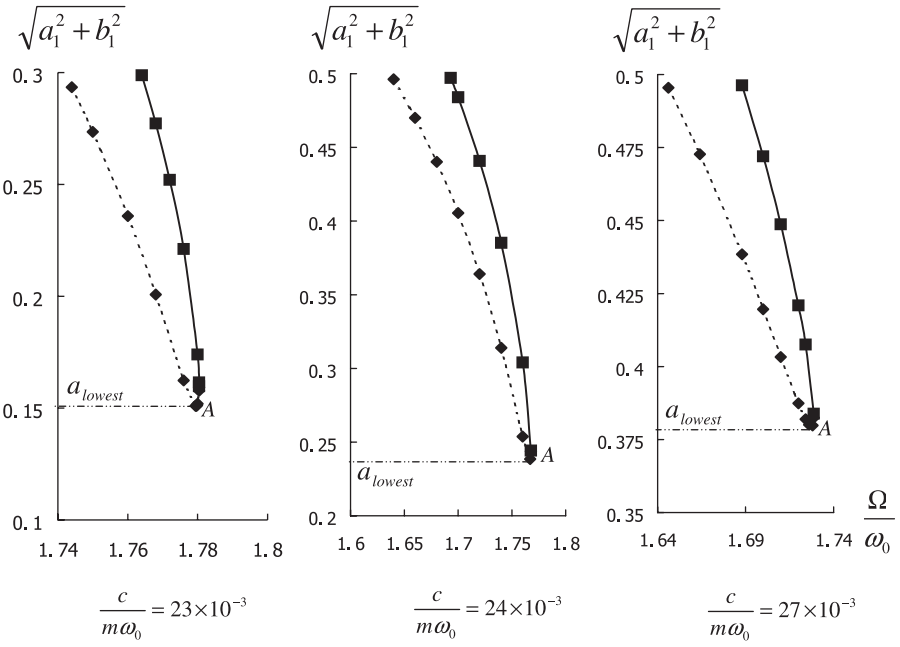

Fig. 5. Parametric resonance for $\lambda = 2$ with the viscous coefficient more than the critical value when $Q = \frac{\varepsilon_0 S V_{dc}^2}{2d_0^3 q} = 1/20$ and $\frac{V_{ac}}{V_{dc}} = 0.1$, where the critical value is $\frac{c}{m\omega_0} = 22.2\times10^{-3}$ for $\lambda = 2$ (solid line: stable steady-state solutions; dashed line: unstable steady-state solutions).

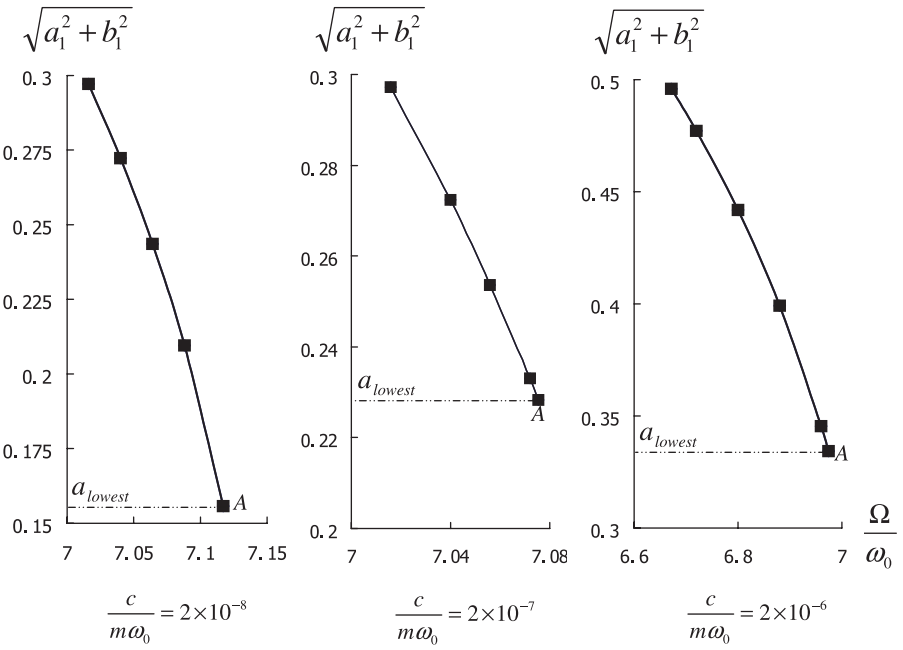

Fig. 6. Parametric resonance for $\lambda = 8$ with the viscous coefficient when $Q = \frac{\varepsilon_0 S V_{dc}^2}{2d_0^3 q} = 1/20$ and $\frac{V_{ac}}{V_{dc}} = 0.1$.

is defined as a_{lowest}, then the lowest amplitude a_{lowest} increases with increasing viscous coefficient. For example, a_{lowest} is $0.159\,d_0$ when the viscous coefficient $\frac{c}{m\omega_0}$ is 23×10^{-3}, while a_{lowest} increases to $0.244\,d_0$ or $0.383\,d_0$ when the viscous coefficient increases to 24×10^{-3} or 27×10^{-3}. Our results show that the responses for $\lambda = 0.5$ and 1 are essentially similar to that shown in Figure 4 or 5 for $\lambda = 2$, and therefore the details for $\lambda = 0.5$ and 1 are not shown here.

In summary, for $\lambda \leqslant 2$, there exists a positive critical value for the viscous coefficient, as shown in Table 1. When the viscous coefficient is less than (or equal to) the critical value, stable periodic solutions with vanishingly small amplitude exist and parametric resonance exhibit similar phenomena as those discussed in Section 3 in the absence of damping. However, when the viscous coefficient is larger than the critical value, the amplitudes of possible stable periodic solutions are bounded from below by the

Table 1. Critical viscous coefficient $\frac{c}{m\omega_0}$ when $Q = \frac{\varepsilon_0 S V_{dc}^2}{2d_0^3 q} = 1/20$ and $\frac{V_{ac}}{V_{dc}} = 0.1$.

λ	0.5	1	2	3	4	8
Critical viscous coefficient $\frac{c}{m\omega_0}$	7.6×10^{-3}	0.56×10^{-3}	22.2×10^{-3}	0	0	0

smallest amplitude a_{lowest} which increases with increasing viscous coefficient. In this case, periodic solutions with amplitude smaller than a_{lowest} will not exist. In particular, because the critical viscous coefficient for$\lambda \geqslant 3$ is always zero (see Tab. 1), high-order subharmonic parametric resonance with vanishing small amplitude will not exist in the presence of any small linear damping.

Here, it should be stated that the damping effect on parametric resonance is a complicated issue. On one hand, Rhoads et al. [19,20] stated that the response is largely unaffected by damping and therefore these authors have limited their attention to linear damping only. On the other hand, Lifshitz and Cross [11] indicated that nonlinear damping is important for the amplitudes of steady-state solutions. In the present study, we only considered a linear damping, and how does a nonlinear damping affect parametric resonance of nonlinearly coupled oscillators requests further research.

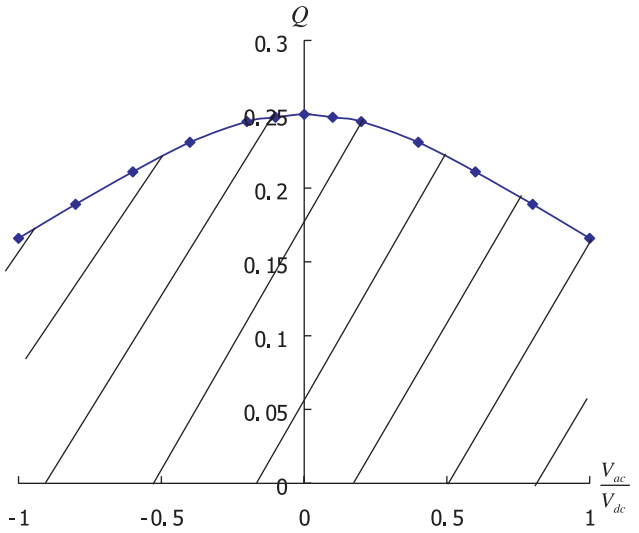

Fig. 7. Domain of Q and $\frac{V_{ac}}{V_{dc}}$ in which non-trivial stable periodic solutions can be obtained for high-order parametric resonance with $\lambda \geqslant 3$ in the absence of damping, where $Q = \frac{\varepsilon_0 S V_{dc}^2}{2d_0^3 q}$.

4.2 Parametric resonance with $\lambda \geqslant 3$

Let us now consider the damping effect on parametric resonance with $\lambda \geqslant 3$. It is found that the critical viscous coefficient for $\lambda \geqslant 3$ is constantly zero, as shown in Table 1, and there exists no periodic solution with vanishingly small amplitude for $\lambda \geqslant 3$ when the viscous coefficient is non-zero. In other words, for non-zero viscous coefficient, the amplitudes of all possible periodic solutions with $\lambda \geqslant 3$ are bounded from below by a positive number.

Figure 6 shows the relationship between the amplitude of the excited stable periodic solution and the ac frequency with non-zero viscous coefficient for $\lambda = 8$. It is seen from Figure 6 that the lowest amplitude a_{lowest} in the solution curve increases as the viscous coefficient increases. For example, the lowest amplitude a_{lowest} is $0.156\,d_0$ when the viscous coefficient $\frac{c}{m\omega_0}$ is 2×10^{-8}, while a_{lowest} increases to $0.228\,d_0$ or $0.334\,d_0$ when the viscous coefficient increases to 2×10^{-7} or 2×10^{-6}. Our results show that the responses for $\lambda = 3$ and 4 are essentially similar to that shown in Figure 6 for $\lambda = 8$, and therefore the details for $\lambda = 3$ and 4 are omitted here.

These results are consistent with the expected stabilizing effects of damping on parametric resonance. In fact, in the presence of a non-zero damping, it is expected that high-order subharmonic parametric resonance could occur only when the disturbances are large enough to bring the oscillator system to one stable steady-state state which is at a finite distance from the equilibrium position. Thus, roughly speaking, there are two conditions for the occurrence of high-order subharmonic parametric resonances with smaller disturbance. The first one is that the viscous coefficient should be reasonably lower, and the second one is that the excitation frequency should be sufficiently close to a multiple ($\geqslant$3) of one of the natural frequencies of the system. In the presence of a sufficiently large damping, high-order subharmonic parametric resonance could occur only when the disturbances are large enough, to offer sufficient energy to drive the oscillator system to one steady-state periodic state which is at a finite distance from the equilibrium position.

Finally, it should be stated that the existence of stable high-order subharmonic parametric resonance also depends on the loading parameter Q and the excitation parameter V_{ac}/V_{dc}. The domain of Q and V_{ac}/V_{dc} in which non-trivial stable steady-state solutions exist for high-order parametric resonance with $\lambda \geqslant 3$, in the absence of any damping, is shown in the shaded area in Figure 7. For example, when $V_{ac}/V_{dc} = 0.1$, the loading parameter Q must be less than 0.248, in order to obtain the stable high-order parametric resonance with $\lambda \geqslant 3$. When V_{ac}/V_{dc} is 0, on the other hand, the problem becomes a static one and the system will become unstable when the loading parameter Q is more than 1/4, consistent with the general results obtained in [29,30] for a large array of coupled springs.

It should be stated here that the results obtained here are applicable not only to coupled microbeams, but also to coupled nanobeams [5,7,8]. For instance, it has been well established that attractive van der Waals interaction between parallel carbon nanotubes often become

the single dominant force in their mechanical deformation, and mechanical behavior of carbon nanotubes, as the most promising building blocks of future NEMS (nanoelectromechanical systems), can be well described by elastic beam models [36–40].

5 Conclusions

Parametric resonance of comb-drive microcantilevers is studied based on a simplified model of nonlinearly coupled micromechanical oscillators. Different than most of previous related works, the present study focuses on the effects of periodically varying nonlinear coupling on parametric resonance, with a particular interest in the existence of high-order subharmonic parametric resonance. Indeed, our results show that the periodically varying nonlinear coupling leads to the occurrence of high-order subharmonic parametric resonance when the excitation frequency is equal or close to a multiple (say 3, 4, 8, or more) of one of the natural frequencies of the oscillator system. These results distinguish the present analysis from most previous related works based on a linearized coupling, and are well consistent with a few earlier theoretical and experimental works conducted for some specific forms of nonlinear coupling. Also, the effect of a linear damping on parametric resonance is investigated, and a critical viscous coefficient is defined as one of the conditions for the occurrence of parametric resonance. It is believed that the results obtained here offer new and interesting insights into the ongoing research on nonlinear dynamics of coupled microbeams or nanobeams in MEMS or NEMS.

Financial support of the Natural Science and Engineering Research Council (NSERC) of Canada is gratefully acknowledged.

Appendix A

Let us use the method of [34] to analyze stability of steady-state solutions for the middle oscillator coupled with two fixed ones described by (5). If the nonlinear coupling terms $1/(1-x_1)^2$ and $1/(1+x_1)^2$ are expanded into a Taylor series up to the 7th power, (5) becomes

$$\frac{d^2x_1}{d\tau^2}+\frac{c}{m\omega_0}\frac{dx_1}{d\tau}+x_1 - Q(4x_1+8x_1^3+12x_1^5+16x_1^7) \times\left[1+2\frac{V_{ac}}{V_{dc}}\cos\left(\frac{\Omega}{\omega_0}\tau\right)+\left(\frac{V_{ac}}{V_{dc}}\right)^2\cos^2\left(\frac{\Omega}{\omega_0}\tau\right)\right]=0. \tag{A.1}$$

Consider a subharmonic solution of order $1/\lambda$ with the form

$$x_1(\tau)=A_m(\tau)\cos[\frac{\Omega}{\lambda\omega_0}\tau-\psi(\tau)]\equiv A_m(\tau)\cos[\theta(\tau)] \tag{A.2}$$

with condition [34]

$$\dot{A}_m\cos\theta+A_m\dot{\psi}\sin\theta=0 \tag{A.3}$$

to ensure $\dot{x}_1(\tau)=-A_m\frac{\Omega}{\lambda\omega_0}\sin\theta$. Substituting (A-2) into (A-1), we obtain

$$-\dot{A}_m\sin\theta+A_m\dot{\psi}\cos\theta-A_m\omega\cos\theta-\frac{c}{m\omega_0}A_m\sin\theta+\frac{A_m\cos\theta}{\omega}-\frac{Q}{\omega}f(A_m\cos\theta,\tau)=0 \tag{A.4}$$

where $\omega=\frac{\Omega}{\lambda\omega_0}$, and

$$f(A_m\cos\theta,\tau)=[4A_m\cos\theta+8(A_m)^3\cos^3\theta+12(A_m)^5\cos^5\theta+16(A_m)^7\cos^7\theta]\times\left[1+2\frac{V_{ac}}{V_{dc}}\cos\left(\frac{\Omega}{\omega_0}\tau\right)+\left(\frac{V_{ac}}{V_{dc}}\right)^2\cos^2\left(\frac{\Omega}{\omega_0}\tau\right)\right].$$

Multiplying (A-3) by $\cos\theta$ and (A-4) by $\sin\theta$, and subtracting, we obtain

$$\dot{A}_m+A_m\omega\sin\theta\cos\theta+\frac{c}{m\omega_0}A_m\sin^2\theta-\frac{A_m\sin\theta\cos\theta}{\omega}+\frac{Q}{\omega}f\sin\theta=0. \tag{A.5}$$

Multiplying (A-4) by $\sin\theta$ and (A-5) by $\cos\theta$, and adding, we obtain

$$A_m\dot{\psi}-A_m\omega\cos^2\theta-\frac{c}{m\omega_0}A_m\sin\theta\cos\theta+\frac{A_m\cos^2\theta}{\omega}-\frac{Q}{\omega}f\cos\theta=0 \tag{A.6}$$

with the slowly varying parameter technique [32,34], $A_m(\tau)$ and $\psi(\tau)$ are considered constant over one cycle. Thus, integrating (A-5) and (A-6) with respect to θ from 0 to 2π, we obtain

$$\dot{A}_m+\frac{c}{2m\omega_0}A_m+\frac{Q}{2\pi\omega}\int_0^{2\pi}f\sin\theta d\theta=0 \tag{A.7}$$

$$A_m\dot{\psi}-\frac{A_m\omega}{2}+\frac{A_m}{2\omega}-\frac{Q}{2\pi\omega}\int_0^{2\pi}f\cos\theta d\theta=0. \tag{A.8}$$

Let $\dot{A}_m=0$ and $\dot{\psi}=0$, we obtain steady-state solutions of specific order λ. These steady-state solutions are exactly same as those obtained with the harmonic balance method with $A_m=\sqrt{a_1^2+b_1^2}$ and $\psi=arctg(b_1/a_1)$. Based on (A-7) and (A-8), we can analyze the stability of these steady-state solutions. For example, when $\lambda=8$ and $c=0$ (without damping), we can obtain the steady-state solutions defined by the following equations

$$\sin(8\psi)=0 \tag{A.9}$$

$$-\frac{\omega}{2}+\frac{1}{2\omega}-2\frac{Q}{\omega}\left(1+0.5\frac{V_{ac}^2}{V_{dc}^2}\right)-3\frac{Q}{\omega}\left(1+0.5\frac{V_{ac}^2}{V_{dc}^2}\right)(A_m)^2$$
$$-3.75\frac{Q}{\omega}\left(1+0.5\frac{V_{ac}^2}{V_{dc}^2}\right)(A_m)^4-4.375\frac{Q}{\omega}\left(1+0.5\frac{V_{ac}^2}{V_{dc}^2}\right)(A_m)^6$$
$$-0.125\frac{Q}{\omega}\frac{V_{ac}}{V_{dc}}\cos(8\psi)(A_m)^6=0. \quad \text{(A.10)}$$

Stability of a steady-state solution, defined by (A-9) and (A-10) with the specific coefficients Q, V_{ac}/V_{dc} and $\frac{\Omega}{\omega_0}$ ($\omega=\frac{\Omega}{8\omega_0}$), can be studied as follows. Let us define

$$A_m=A_m^0+\varepsilon, \quad \psi=\psi^0+\eta \quad \text{(A.11)}$$

where A_m^0 and ψ^0 are the solution of (A-9) and (A-10), and ε and η are infinitesimal disturbance in the neighborhood of (A_m^0, ψ^0) in the $A_m-\psi$ phase plane. For example, because A_m^0 and ψ^0 satisfy (A-9) and (A-10), substituting (A-11) into (A-7) and (A-8) with $\lambda=8$ and $c=0$ and retaining only the first power of ε and η, we obtain

$$\dot{\varepsilon}=\frac{Q}{\omega}\frac{V_{ac}}{V_{dc}}(A_m^0)^7\cos(8\psi^0)\eta \quad \text{(A.12)}$$

$$A_m^0\dot{\eta}+\varepsilon\Bigg[-\frac{\omega}{2}+\frac{1}{2\omega}-2\frac{Q}{\omega}\left(1+0.5\frac{V_{ac}^2}{V_{dc}^2}\right)$$
$$-9\frac{Q}{\omega}\left(1+0.5\frac{V_{ac}^2}{V_{dc}^2}\right)(A_m^0)^2-18.75\frac{Q}{\omega}\left(1+0.5\frac{V_{ac}^2}{V_{dc}^2}\right)(A_m^0)^4$$
$$-30.625\frac{Q}{\omega}\left(1+0.5\frac{V_{ac}^2}{V_{dc}^2}\right)(A_m^0)^6-\frac{7}{8}\frac{Q}{\omega}\frac{V_{ac}}{V_{dc}}\cos(8\psi^0)(A_m^0)^6\Bigg]=0. \quad \text{(A.13)}$$

Substituting (A-12) into (A-13), we obtain

$$\ddot{\eta}+g(A_m^0,\psi^0)\eta=0 \quad \text{(A.14)}$$

where

$$g(A_m^0,\psi^0)=\frac{Q}{\omega}\frac{V_{ac}}{V_{dc}}(A_m^0)^6\cos(8\psi^0)\Bigg[-\frac{\omega}{2}+\frac{1}{2\omega}$$
$$-2\frac{Q}{\omega}\left(1+0.5\frac{V_{ac}^2}{V_{dc}^2}\right)-9\frac{Q}{\omega}\left(1+0.5\frac{V_{ac}^2}{V_{dc}^2}\right)(A_m^0)^2$$
$$-18.75\frac{Q}{\omega}\left(1+0.5\frac{V_{ac}^2}{V_{dc}^2}\right)(A_m^0)^4$$
$$-30.625\frac{Q}{\omega}\left(1+0.5\frac{V_{ac}^2}{V_{dc}^2}\right)(A_m^0)^6$$
$$-\frac{7}{8}\frac{Q}{\omega}\frac{V_{ac}}{V_{dc}}\cos(8\psi^0)(A_m^0)^6\Bigg]. \quad \text{(A.15)}$$

Thus the steady-state solutions with $g(A_m^0,\psi^0)>0$ are stable, while those with $g(A_m^0,\psi^0)<0$ are unstable. For large disturbances, we can use equations (A-7) and (A-8) to plot the trajectories in the $A_m-\psi$ phase plane to analyze the nature of the point (A_m^0, ψ^0). Our results show that for $\lambda=8$ and $c=0$, the solutions with $\cos(8\psi^0)=-1$ are stable, while the solutions with $\cos(8\psi^0)=1$ are unstable. Stability of the steady-state solutions with $\lambda=0.5$, 1, 2, 3, 4 can be analyzed in a similar way.

References

1. N. Tas, T. Sonnenberg, H. Jansen, R. Legtenberg, M. Elwenspoek, Stiction in surface micromachining, J. Micromech. Microeng. **6**, 385 (1996)
2. R. Maboudian, R.T. Howe, J. Vac. Sci. Technol. **B15**, 1 (1997)
3. C.H. Mastrangelo, Tribol. Lett. **3**, 223 (1997)
4. *Springer handbook of nanotechnology.* edited by B. Bhushan (Springer, Berlin, 2004)
5. H.G. Craighead, Nanoelectromechanical systems, Science **290**, 1532 (2000)
6. M.L. Roukes, Phys. World **14**, 25 (2001)
7. C. Hierold, J. Micromech. Microeng. **14**, S1-11 (2004)
8. K.L. Ekinci, M.L. Roukes, Rev. Sci. Instrum. **76**, 061101 (2005)
9. E. Buks, M.L. Roukes, Europhys. Lett. **54**, 220 (2001)
10. E. Buks, M.L. Roukes, J. Microelectromech. Syst. **11**, 802 (2002)
11. R. Lifshitz, M.C. Cross, Phys. Rev. B **67**, 134302 (2003)
12. Y. Bromberg, M.C. Cross, R. Lifshitz, Phys. Rev. E **73**, 016214 (2006)
13. M. Zalalutdinov, B. Ilic, D. Czaplewski, A. Zehnder, H.G. Craighead, J.M. Parpia, Appl. Phys. Lett. **77**, 3287 (2000)
14. M. Sato, B.E. Hubbard, A.J. Sievers, B. Ilic, D.A. Czaplewski, H.G. Craighead, Observation of locked intrinsic localized vibrational modes in a micromechanical oscillator array, Phy. Rev. Lett. **90**, 044102 (2003)
15. M. Sato, B.E. Hubbard, L.Q. English, A.J. Sievers, B. Ilic, D.A. Czaplewski, H.G. Craighead, Chaos **13**, 702 (2003)
16. M. Sato, B.E. Hubbard, A.J. Sievers, Rev. Mod. Phys. **78**, 137 (2006)
17. M. Sato, B.E. Hubbard, A.J. Sievers, B. Ilic, H.G. Craighead, Europhys. Lett. **66**, 318 (2004)
18. S. Flach, C.R. Willis, Phys. Rep. **295**, 181 (1998)
19. J.F. Rhoads, S.W. Shaw, K.L. Turner, J. Micromech. Microeng. **16**, 890 (2006)
20. J.F. Rhoads, S.W. Shaw, K.L. Turner, J. Moehlis, B.E. DeMartini, W. Zhang, J. Sound Vib. **296**, 797 (2006)
21. I. Bena, C.V.D. Broeck, Europhys. Lett. **48**, 498 (1999)
22. D. Goldobin, A. Pikovsky, Europhys. Lett. **59**, 193 2002
23. R.V. Bobryk, A. Chrzeszczyk, Europhys. Lett. **68**, 344 (2004)
24. J.A. Pelesko, D.H. Bernstein, *Modeling MEMS and NEMS* (Chapman & Hill/CRC, Boca Raton, FL, 2003)
25. T. Harness, R.A. Syms, J. Micromech. Microeng. **10**, 7 (2000)
26. J.D. Grade, H. Jerman, T.W. Kenny, J. Microelectromech. Syst. **12**, 335 (2003)
27. G.Y. Zhou, P. Dowd, J. Micromech. Microeng. **13**, 178 (2003)
28. T.L. Sounart, T.A. Michalske, K.R. Zavadil, J. Microelectromech. Syst. **14**, 125 (2005)
29. J. Zhu, C.Q. Ru, A. Mioduchowski, J. Micromech. Microeng. **16**, 2220 (2006)

30. J. Zhu, C.Q. Ru, A. Mioduchowski, J. Adhes. Sci. Technol. **20**, 1125 (2006)
31. N.W. Mclachlan, *Theory and Application of Mathieu Functions* (Dover, New York, 1964)
32. A.H. Nayfeh, D.T. Mook, *Nonlinear Oscillation* (Wiley, New York, 1979)
33. N.A. Bobylev, Y.M. Burman, S.K. Korovin, *Approximate procedures in nonlinear oscillation theory* (Walter de Gruyter, Berlin, 1994)
34. W.K. Tso, T.K. Caughey, J. Appl. Mech. – T. ASME **32**, 899 (1965)
35. M. Mond, G. Cederbaum, P.B. Khan, Y. Zarmi, J. Sound and Vib. **167**, 77 (1993)
36. M.M. Treacy, T.W. Ebbesen, J.M. Gibson, Nature (London) **381**, 678 (1996)
37. E.W. Wong, P.E. Sheehan, C.M. Lieber, Science **277**, 1971 (1997)
38. P. Poncharal, Z.L. Wang, D. Ugarte, W.A. de Heer, Science **283**, 1513 (1999)
39. M. Dequesnes, S.V. Rotkin, N.R. Aluru, Nanotechnology **13**, 120 (2002)
40. C.Q. Ru, *"Elastic models for carbon nanotubes"* in *Encyclopedia of Nanoscience and Nanotechnology*, edited by H.S. Nalwa (American Scientific Publishers, 2004) Vol. 2, pp. 31–744